Hovi A., Raitio P., Rautiainen M. (2017). A spectral analysis of 25 boreal tree species. Silva Fennica vol. 51 no. 4 article id 7753. https://doi.org/10.14214/sf.7753

Supplement **S**1: Technical description of coniferous needle measurements

1. Integrating sphere and measurement protocol

An RTS-3ZC integrating sphere and a CL-10 (10 W) halogen light source by Analytical Spectral Devices (ASD) Inc. (Fig. 1) were used in the coniferous needle measurements. We used the standard measurement protocol (comparison mode) recommended by ASD (ASD Inc. 2008). In addition, special needle carriers were used to hold the needles during measurements (Fig. 1F; Malenovský et al. 2006; Yanez-Rausell et al. 2014). The carriers were manufactured from steel plates and painted with Nextel® Suede Coating paint (7329 S139 'dark black'). During the measurements, the needles were placed in between two carriers so that the distance between needles was 0.5–1 times the thickness of the needle. Thus, the gap fractions in the samples varied from 33% to 50%. The needles were attached to the carriers either from both tips, if they were longer than the diameter of the carrier's opening (16 mm), or from one tip only (two rows) if they were shorter.

The measurement of a needle sample consisted of reflectance, transmittance, reference and stray light readings, which were acquired with an ASD FieldSpec 4 spectrometer, using an integration time of 1.09 s per measurement and averaging 30 measurements for one reading. The measurement protocol, including placement and thickness of the needle carriers, is described in Table 1. In addition, dark current was manually measured after each sample, by taking a reading while the detector fiber of the spectrometer was capped with a black rubber. The dark current was subtracted from all spectrometer readings before further processing.

After all measurements had been conducted, it turned out that the integrating sphere that was used in the measurements had been partly defectively manufactured. The company designing and selling the sphere (ASD Inc.) also confirmed and admitted this error. The interior of the black metal plates around sample ports B and C (the 15 mm wide area seen in Fig. 1B, C) were not painted in white as they should be. This caused attenuation of the signal in measurements that involved direct scattering from either sample or white reference in ports B and C (i.e., measurements #1–3 and #5 in Table 1). The average thicknesses of the metal plates were 2.5 mm for port B, and 1.3 mm for port C. Thus, they caused attenuation that was similar in magnitude compared to the effect of needle carriers (thickness of 1.6–1.7 mm). For reflectance measurements (#1–3) the effect was minor, because attenuation was the same for both reflectance and reference readings, and thus did not influence the computed reflectance values notably. For transmittance measurements the effect was larger, but it was partly compensated for by the needle carrier. The needle carrier was used for holding the sample (measurements #6–7 in Table 1), but was not placed in front of the white reference (port B) when performing the reference measurement (#5 in Table 1). To assess the combined effect of defective sphere and needle carriers, we measured samples

of white paper with a) a repaired sphere (that had all ports painted in white) without needle carriers, b) defective sphere with needle carriers. The relative difference in reflectance was below 3%, and in transmittance below 12%. These values are comparable to overall uncertainties associated with optical properties measurements of coniferous needles reported by Yanez-Rausell et al. (2014) (4–6% for reflectance, 10–12% for transmittance). Thus, we can conclude that the measurements were reliable, and most importantly, followed exactly the same protocol throughout the campaign, which means that the results are internally consistent.

Figure 1. Pictures of ASD integrating sphere and its sample ports. A-E: Closeups of the sample ports A-E. F: A picture of the sphere with a needle carrier in port C (same configuration as in reflectance measurements, #2–3 in Table 1).

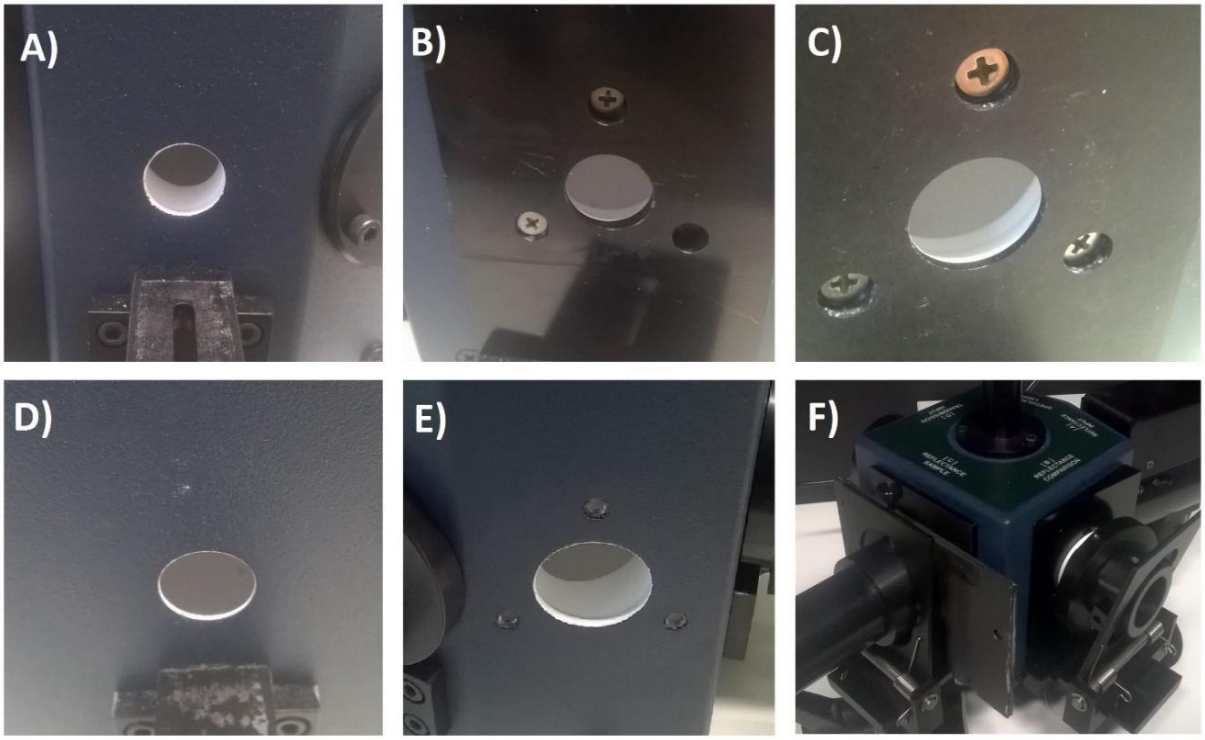

Table 1. Measurement protocol and port configuration in the integrating sphere in needle measurements. L = lamp, S = sample, C = needle carrier, T = photon trap, W = reference target (99% reflective Spectralon®), P = Spectralon® plug. Thickness of the needle carrier, i.e. distance between the sample and the outer surface of the sphere wall, is given in millimeters. Note that for needle samples the total carrier thickness is double the announced (i.e. 3.4 mm), because the needle sample is held in between two carriers.

		Port A	Port B	Port C	Port D	Port E
			Reflectance mode			
1	White reference	L	S + C (1.7) + T	W + C (1.6)	P	P
2	Reflectance, adaxial	L	W + C (1.6)	S + C (1.7) + T	P	P
3	Reflectance, abaxial	L	W + C (1.6)	S + C (1.7) + T	P	P
4	Stray light	L	W + C (1.6)	C (1.6) + T	P	P
			Transmittance mode			
5	White reference	P	W	S + C (1.7) + T	L + C (1.6)	P
6	Transmittance, adaxial	P	W	C (1.6) + T	L + S + C (1.7)	P
7	Transmittance, abaxial	P	W	C (1.6) + T	L + S + C (1.7)	P
8	Stray light	P	C (1.6) + T	W	L + C (1.6)	P

2. Determining gap fractions in the needle samples

After measuring a sample, the carrier with the sample was scanned on both sides, using a photo scanner (Epson Perfection V550 Photo) in a film scanning mode, i.e. the sample was illuminated from the other side and scanned from the other. Gaps were detected by thresholding the scanned 8-bit black-and-white image. First, digital masks were prepared by carefully measuring the size and position of the illuminating light beam in relation to the carrier in each measurement configuration (#2–3 and #6–7 in Table 1). Second, thresholding was performed for the masked image to determine the gap fraction of the sample inside the light beam. We used a threshold of 240 in our measurements, based on the following reasoning. First, it was assumed that when image resolution is very high, no mixed pixels are present and pure white pixels represent background. The value of 240 (the maximum i.e. pure white is 255) was chosen as a compromise that minimized noise caused by impurities in the background. Image resolution was then reduced from the maximal value (3200 dpi) until the gap fraction estimates started to decrease at values lower than 800 dpi due to significant proportion of mixed pixels (background and sample). We therefore used resolution of 800 dpi in all our measurements.

3. Equations for calculating reflectance and transmittance

Total reflectance and transmittance (ρ_{total}, τ_{total}) of the needle sample, including gaps between the needles, were calculated with following equations:

$$r_{total} = \frac{I_{sample,R} - I_{str,R}}{I_{ref,R} - I_{str,R}} \cdot R_{ref} \quad (1)$$

$$t_{total} = \frac{I_{sample,T}}{I_{ref,T} - I_{str,T}} \cdot R_{ref} \quad (2)$$

where I_{sample}, I_{ref}, and I_{str} are the spectrometer readings (digital numbers) recorded for sample, white reference, and stray light, respectively, and R_{ref} is the reflectance factor of the white reference (99% reflective Spectralon®). Subscripts R and T refer to measurements in reflectance and trasmittance mode, respectively. Values of ρ_{total} and τ_{total} were corrected for gap fractions (GF) to yield reflectance and transmittance (ρ, τ) of the sample, using the following formulas (Mesarch et al. 1999):

$$r = \frac{r_{total}}{1 - GF} \quad (3)$$

$$t = \left(t_{total} - R_{ref} GF\right)\frac{1}{1 - GF} \quad (4)$$

References

ASD Inc. 2008. Integrating sphere user manual. ASD Document 600660 Rev. B.

Malenovský Z., Albrechtova J., Lhotáková Z., Zurita-Milla R., Clevers J., Schaepman M., Cudlín P. (2006). Applicability of the PROSPECT model for Norway spruce needles. International Journal of Remote Sensing 27: 5315–5340.

Mesarch M.A., Walter-Shea E.A., Asner G.P., Middleton E.M., Chan S.S. (1999). A revised measurement methodology for conifer needles spectral optical properties - evaluating the influence of gaps between elements. Remote Sensing of Environment 68: 177–192.

Yanez-Rausell L., Malenovský Z., Clevers, G.P.W., Schaepman, M.E. (2014). Minimizing Measurement Uncertainties of Coniferous Needle-Leaf Optical Properties, Part II: Experimental set-up and error analysis IEEE Journal of Selected Topics in Applied Earth Observation and Remote Sensing 7: 1–15.